P1.1 USE OF SATELLITE CLOUD CLIMATOLOGY FOR ASSESSING CLOUD-FREE-LINE-OF-SIGHT PROBABILITIES

Ray Hobbs*, J. Mitchell, M. A. Bedrick, D. J. Rusk and R. L. Rose
Aeromet, Inc., Tulsa OK

1. INTRODUCTION

Clouds that block the view of airborne optical sensors are always a source of concern. Methods for assessing the probability of a Cloud-Free Line-Of-Sight (**CFLOS**) between a sensor and phenomena being observed are of interest in many applications. Experiment planners managing airborne assets would benefit from knowledge of the horizontal and vertical climatology of clouds to maximize the probabilities of successful data collection. A methodology has been developed to apply this method at different locations.

The problem can be phrased as a question—"What is the probability that an airborne sensor at some altitude and location will have a cloud-free line-of-sight to an object of interest?" This question can be addressed by using a unique data set compiled at the Space Science and Engineering Center (**SSEC**) at the University of Wisconsin [Wylie and Menzel (1989, 1999) and Wylie et al. (1994)]. Satellite data has been used to compile a global cloud climatology that is used to calculate the probabilities of viewing based on the airborne sensor's altitude and the viewing path.

The satellite data set used in the study is discussed, and the algorithm used to calculate the probabilities is explained. Results for the Kwajalein Island area in the central Pacific, Barrow, AK and Lamont OK are shown.

2. HIRS DATA

A worldwide cloud top height climatology has been composed by Wylie and Menzel (1989, 1999) and Wylie et al. (1994)[1]. The data, compiled since 1989, is from the High-Resolution Infrared Radiation Sounder (**HIRS**) on the National Oceanic and Atmospheric Administration -10, -11, -12, -14 and -15 polar orbiting earth satellites. The HIRS sensor is one of three instruments in the Television Infrared Observation Satellite Operational Vertical Sounder.

A technical discussion of the algorithms used for cloud height computations may be found in Wylie et al. (1994). Wylie's climatology samples every third line of data from every third HIRS Field of View. Data are taken from 10º each side of nadir. Basically, cloud top pressures and "clear" pixels are calculated from the HIRS infrared bands with partial carbon dioxide ($\mathbf{CO_2}$) absorption (13 to 15 microns (μ**m**) wavelength), from the "window" channel (11.1 μm), and from the water vapor channel (8.3 μm). First, a pixel is either found to be "clear" or to contain clouds. If the pixel is clear, it is marked as so. If it is not clear, the cloud top pressure and effective emissivity ($\mathbf{N\varepsilon}$) of the detected cloud are calculated. Nε can be thought of as the product of the fractional cloud coverage in a pixel (**N**) and the emissivity ($\boldsymbol{\varepsilon}$). The individual components cannot be directly measured.

The fact that Nε is actually what is measured, rather than just ε, is a consequence of making that measurement from an element with a cross-sectional area. The satellite cannot tell if a pixel is half-covered (N = 0.5) with perfectly opaque clouds (ε = 1.0) or totally covered (N = 1.0) with clouds that have ε = 0.5. The same value, 0.5, is measured in each instance.

The globe for the climatology is divided into 2º (latitude) × 3º (longitude) areas (from 82º S to 82º N) with 18 levels in the vertical. The lowest altitude bin starts at 0.5 km and extends to 1.99 km. All others are 1 km in depth. The data therefore extend from .5 to 18.99 km. Nε values are sorted as being ≥ 0.1, ≥ 0.3, ≥ .6, ≥ 0.9, and ≥ 0.95. The cloud top altitude and Nε range value for each pixel that falls within the larger climatology volume element contributes to the final frequency distribution of cloudiness.

The final climatology contains top-down vertical cumulative frequencies of Nε within these volumes. In the data used by Aeromet, the cumulative frequency of clouds with Nε ≥ 0.1 is used. Counting clouds with Nε ≥ 0.1 takes into account all detected clouds, no matter how optically "thin" they are.[2] For comparison, the solar disk would be visible through clouds with Nε ≥ 0.3. At Nε ≥ 0.6, clouds become opaque to atmospheric lidars and the sun would appear as a bright spot in a cloud. With Nε ≥ 0.95, the cloud would be completely opaque and the solar disk would be lost.

Some of the characteristics of this data set should be noted. Because the climatology uses only data sampled from zenith angles of less than 10º, high altitude cloud amounts are probably underestimated (Rose *et al*., 2001). Although the maximum altitude at which clouds are found varies over the globe, the upper level at which cloud top calculations are made will never exceed 18.99 km. It is unknown whether or not clouds could be sampled at or above that level. The altitude that best explains the satellite measurements based on solutions of the radiative transfer equations is assigned to be the cloud top. Therefore, even though there may be readings from other clouds in a vertical array of pixels, only that datum assigned to one cloud top is kept.

* *Corresponding author address:* Dr. Ray Hobbs, Aeromet, Inc., PO Box 701767, Tulsa OK 74137; e-mail rhobbs@aeomet.com

[1] These three papers will be collectively referred to as Wylie.

[2] There are no cloud tops from Nε < .1, although clouds may be present at these small values. Therefore, the amount of cloudiness may be underestimated in the climatology, which may be significant in affecting CFLOS probabilities over long atmospheric path lengths.

Layers above that containing the assigned cloud top are considered clear; layers below are not considered. Cloud frequency calculations take into account the fact that not all levels in the vertical are considered to be sampled in each observation. For example, clouds may exist in layers below a cloud deck to which the cloud top is assigned; however, they are not considered to be sampled and the "null" observations in those layers are not part of the statistical calculations.

The percentage of clouds measured with $N\varepsilon \geq 0.1$, for the atmospheric volume over the Kwajalein Atoll are shown in **Figure 1**. Several features are of interest here; for example, the distinct drop in the percentage of occurrence of $N\varepsilon \geq 0.1$ in the lower 11 km or so in the dry season (roughly February – April) and in this percentage in the same layers in the rainy season (roughly August-October). The upper layers (above 11 km or so) seem not to vary much with the seasons. However, values there are small. There does seem to be a tendency for the percentage of occurrence of $N\varepsilon \geq 0.1$ to decrease in the highest levels in the rainy season and increase in the dry season, indicating less cloudiness at upper levels in the rainy season and more in the dry. This could be false, and indicative of the algorithm used to locate cloud tops. Once thicker cloud is detected in the lowest layers in the rainy season, higher-level cloud will be counted as clear.

Wylie's data set provides a unique and unsurpassed database for global cloud amount estimations even though there are limitations. The HIRS data are obtained from polar orbiting satellites which sample data independently of the weather. There is a difference in the frequency at which points are sampled due to satellite pass frequency differences from the poles to the equator. Wylie's relatively coarse data set compares favorably to higher resolution data sets (Bedrock et al., 2001). However, the occurrence of high clouds (above 12.5 km) is 20-30% greater in the fine resolution retrieval. This may partly be due to the use of limb data where high cloud top retrievals are more efficient.

3. METHOD

A sample of the data used in this study is in **Table 1**. This annually- averaged data is from the atmospheric column over Kwajalein Island in the Republic of the Marshall Islands. Data from Kwajalein are used in this example because the frequent occurrence of clouds there adversely affects airborne sensors. The goal is to estimate the probability that a sensor at some altitude will be able to observe an object without obscuration due to cloud. We start with the climatology of cloud top heights in 2° (latitude) by 3° (longitude) bins with all but the lowest bin having vertical depths of 1 km. The lowest bin has a depth of .49 km. At the latitude of Kwajalein, the bins are approximately 222 km in the meridional direction and approximately 328 km in the zonal. The estimate of the fraction of occurrence of cloud in each vertical layer (or bin) is used to estimate the fraction of occurrence of cloud-free conditions in each bin. Following that, CFLOS probabilities through each bin are estimated.

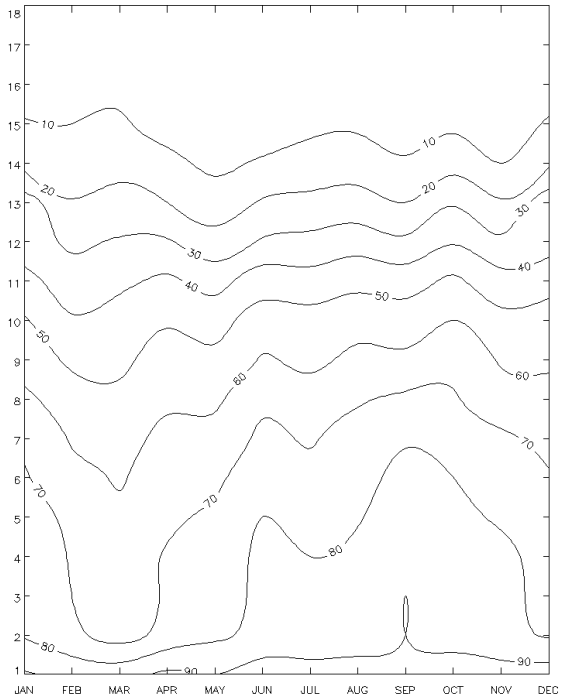

Figure 1: Annual Percentage of Clouds Measured with $N\varepsilon \geq 0.1$ for the Atmospheric Column (2º lat by 3º lon) over Kwajalein.

It is assumed that each bin's characteristics are uniform throughout its volume. This enables calculation of the effects on viewing when a sensor is at some altitude that is within a bin, and we assume that the cloud-free fraction determined from vertical measurements have the same values horizontally.

The key variable is in the third column in **Table 1**, the vertical cumulative fraction of the occurrence of clouds with $N\varepsilon \geq 0.1$, which we call F_h. Any bin with $N\varepsilon$ less than 0.1 is treated as cloud-free. Using the smallest value of $N\varepsilon$ available from Wylie's data set ensures the inclusion of tenuous clouds in the samples. This is done because their effect on viewing is significant.

Subtracting F_h from 1 gives the cloud-free fraction of the column. This is F'_h, and is in the fourth column in **Table 1**. So, F'_h estimates the amount of time the sky is clear, or, stated another way, it is used as the probability of a CFLOS straight up through the volume and out into space. Therefore, looking at **Table 1**, we can say that the probability of having a CFLOS from bin 8 (observer at 8 km) straight up through level 18 and out into space is 0.371 on any random viewing. For the viewings to be random, the time between viewings has to be sufficiently long for the cloud conditions to be uncorrelated.

BIN No.	HEIGHT RANGE (Km)	CUMULATIVE FRACTION OF CLOUD OCCURRENCE (F_h)	CUMULATIVE FRACTION OF CLOUD-FREE OCCURRENCE (F'_h)	SINGLE-BIN CLOUD-FREE PROBABILITY (f'_h)
18	18 – 18.99	.0000	1.00	1.00
17	17 – 17.99	.0108	.989	.989
16	16 – 16.99	.0450	.955	.965
15	15 – 15.99	.0775	.923	.966
14	14 – 14.99	.1333	.867	.939
13	13 – 13.99	.2375	.763	.880
12	12 – 12.99	.3233	.677	.887
11	11 – 11.99	.4325	.568	.839
10	10 – 10.99	.5167	.483	.852
9	9 – 9.99	.5717	.428	.886
8	8 – 8.99	.6292	.371	.866
7	7 – 7.99	.6833	.317	.854
6	6 – 6.99	.7175	.283	.892
5	5 – 5.99	.7525	.248	.876
4	4 – 4.99	.7792	.221	.892
3	3 – 3.99	.7858	.214	.970
2	2 – 2.99	.7958	.204	.953
1	.5 – 1.99	.9258	.074	.363
0	.0 – 0.49	.9258	.074	1.00

Table 1: Annually Averaged Cloud Climatology Data (Nε ≥ 0.1) from Atmospheric Column (2º lat by 3º lon) over Kwajalein Atoll

As noted earlier, the first occurrence of cloud in a column is noted as the cloud top; all bins below that level are disregarded. This is shown in **Figure 2** where n is the occurrence of cloud at a given level.

Specifically the values of n have the following meanings:

n_o is the number of observations where there was no cloud having Nε ≥ 0.1 detected anywhere in the atmosphere from 18.99 down to 0.5 km. This bin does not collect the occurrences of cloud in the height range between 0 and 0.49 km. This height range is excluded in this study.

n_1 is the number of observations where clouds in the vertical column from 18.99 down to 0.5 km were only detected in the layer between 0.5 and 1.99 km. This bin is larger than the rest of the bins.

n_2 is the number of observations where clouds in the vertical column from 18.99 down to 2.00 km were only detected in the layer between 2.00 and 2.99 km. If a cloud was detected in this bin then the presence or absence of any clouds below 2.00 km are ignored.

n_i is the number of observations where clouds in the vertical column from 18.99 down to i km were only detected in the layer between i and i+0.99 km. If a cloud was detected in this bin then the presence or absence of any clouds below i km are ignored.

n_{18} is the number of observations where clouds were detected in the vertical layer between 18.00 and 18.99 km. If a cloud was detected in this bin then the presence or absence of any clouds below 18.00 km are ignored. No clouds having Nε ≥ 0.1 were detected in this bin.

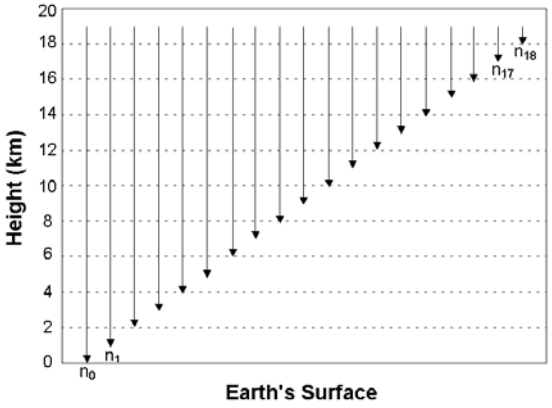

Figure 2: Schematic of the number of occurrences (n) of the detection of Nε ≥ 0.1 as a function of height (h).

Equations are developed that are used to estimate CFLOS probabilities. The fraction (f_h) of cloud observations at a given layer (h), which extends from h to h+0.99 km, is defined by the number of cloud observations in that layer (n_h) divided by the sum of the total observations in that layer and below and is given as follows:

$$f_h = \frac{n_h}{\sum_{i=0}^{h} n_i} \quad (1)$$

The fraction (f'_h) of cloud-free observation in a given layer (h) is therefore:

$$f'_h = 1 - f_h \tag{2}$$

The cumulative fraction (F_h) of cloud observations from the highest layer considered (18.00 - 18.99 km) down to a level h is given by the cumulative number of cloud observations ($n_{18} + n_{17} + \ldots + n_H$) divided by the total number of observations ($n_{18} + n_{17} + \ldots + n_0$) and is given as follows:

$$F_h = \frac{\sum_{i=h}^{18} n_i}{\sum_{i=0}^{18} n_i} \tag{3}$$

Fh is given in Table 1. The denominator of equation 3 is the total number (N) of satellite observations:

$$N = \sum_{i=0}^{18} n_i \tag{4}$$

The fraction of cloud observations in layer h to h+0.99 km ($\hat{f}_h$) out of the total number of observations (N) is given by:

$$\hat{f}_h = \frac{n_h}{N} = \frac{\sum_{i=h}^{18} n_i - \sum_{i=h+1}^{18} n_i}{N} = F_h - F_{h+1}$$

The cumulative fraction of a cloud-free column (F'_h) from h to 18.99 km is (1 - F_h:).

$$F'_h = 1 - F_h \tag{5}$$

F'_h is given in Table 1. If the presence or absence of cloud in each 1 km-deep layer of the atmosphere is independent of the other then F'_h is also given by:

$$F'_h = f'_h \bullet f'_{h+1} \bullet f'_{h+2} \bullet \ldots \bullet f'_{18} = \prod_{j=h}^{18} f'_j \tag{6}$$

where the fraction of occurrence of cloud-free observations (f'_j) is now interpreted to be the probability that a given 1 km-deep layer between j and j + 0.99 km is cloud-free.

Using this assumption, the probability that any given vertical layer of the atmosphere is cloud-free (f'_h) between h and h + 0.99 km can be obtained from the cumulative fraction (F_h) of cloud observations as follows:

$$f'_h = \frac{F'_h}{F'_{h+1}} = \frac{1 - F_h}{1 - F_{h+1}} \tag{7}$$

f'_h is given in Table 1. Therefore given information about the cumulative fraction of cloud in a column of the atmosphere, we can determine the probability that a given vertical section of the atmosphere is cloud-free (f'_h). Equation 8 is equivalent to equation 2 as given below:

$$f'_h = \frac{1 - F_h}{1 - F_{h+1}} = \frac{\sum_{i=0}^{18} n_i - \sum_{i=h}^{18} n_i}{\sum_{i=0}^{18} n_i - \sum_{i=h+1}^{18} n_i} = \frac{\sum_{i=0}^{h-1} n_i}{\sum_{i=0}^{h} n_i}$$

$$= \frac{\sum_{i=0}^{h} n_i - \sum_{i=0}^{h} n_i + \sum_{i=0}^{h-1} n_i}{\sum_{i=0}^{h} n_i} = 1 - \frac{n_h}{\sum_{i=0}^{h} n_i} = 1 - f_h$$

Some of the values in **Table 1** are plotted in **Figure 3**. The cumulative fraction of cloud (F_h, solid line) drops rapidly from bin 1 (0.5 – 1.99 km) to bin 2 (2 – 2.99 km) indicating the presence of a lot of cloud in this layer and also may be the result of this bin being 0.5 km larger the other 17 bins. The cumulative fraction of the cloud-free samples (F'_h) varies as 1- F_h. (equation 5). The single-bin cloud-free probability (f'_h) is low in the lowest layer due to the presence of a high fraction of occurrence of cloud, but varies between 0.83 and 1.0 for heights greater than 2 km.

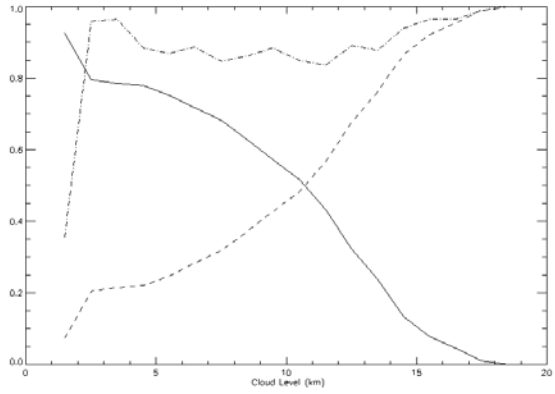

Figure 3: Cumulative Fraction of Cloud Amount (F_h) Versus Height (Solid Line), Cumulative Fraction of the Cloud-Free Column (F'_h) Versus Height (Dashed Line), and Single-Bin Cloud-Free Probability (f'_h) Versus Height (Dash-dot Line) for Annual Mean Kwajalein Data taken from Table 1. (Values are plotted at the mid point of a given bin.)

We want to generalize the method to include all viewing angles. For example, say we are flying along at 12 km

(39,372 ft) and we look vertically; our data in Table 1 indicates that we have a 68% chance of seeing blue sky above us (F'_h) or a 32% chance that we will experience some cloud obscuration(F_h). A simplistic argument is that 32% of the time there are clouds and 68% of the time it is cloud-free (given enough time between samples to ensure randomness). If the atmosphere is either cloudy or clear then looking in directions other than straight up will not change the cloud obscuration.

Experience in Kwajalein indicates this is not the case, that is, it can be clear at one location but cloudy 50 km away at the same height. Therefore, we believe that a correction to cloud obscuration for horizontal viewing is necessary. The problem is to come up with a scheme that properly corrects for the decrease in probability of seeing an object as the viewing path becomes more horizontal.

The initial approach is to introduce the concept of a characteristic length scale (λ). This scale is the distance required for the correlation (r) between the occurrence or absence of cloud is zero between two locations where the presence of cloud is being measured. The characteristic length scale is expected to be significantly different for vertical displacements (λ_v) as compared to horizontal displacements (λ_H).

Dealing initially with the vertical probability of the CFLOS we can generalize equation 7 to allow for vertical viewing through the atmosphere from within a bin, thus giving the CFLOS probability as follows:

$$P'_v = \prod_{i=0}^{18} \left(f'_i\right)^{z_i/\lambda_v} \tag{8}$$

where f'_i is the probability of the absence of cloud in the layer between i and i+0.99 km, z_i is the distance that we are viewing vertically through the layer between i and i+0.99 km and λ_v is taken to have a value of 1 km. λ_v is not expected to have a value of 1 km but is assigned this value because that is the vertical resolution of the data.

Likewise the CFLOS probability for horizontal viewing could be given by:

$$P'_H = \prod_{i=0}^{18} \left(f'_i\right)^{x_i/\lambda_H} \tag{9}$$

where f'_i is the probability of the absence of cloud in the layer between i and i+0.99 km. Irrespective of the viewing being vertical or horizontal, x_i is the distance that we are viewing horizontally through the layer between i and i+0.99 km, and λ_H is the horizontal characteristic length scale. The value of λ_H is unknown. However, a range in λ_H can be hypothesized to be from the size of tropical storms down to the spacing of ocean cumulus clouds. Possibly, λ_H can be considered as follows:

$$\lambda_H = f_1\left(Lat, Long, h, t\right)$$

where f1 is a function of the geographic location (latitude and longitude), h is the height in the atmosphere, t is the time of year. Conceptually we are treating λH is as a length scale in a correlation function:

$$r^2 = f_2\left(x/\lambda_H\right)$$
$$r^2\left(0\right) = 1$$
$$r^2\left(1\right) \cong 0$$

where x is the horizontal distance from the sensor along the viewing path length. For predicting CFLOS probability (P') we need to know the horizontal spacing before we have statistically independent cloud samples.

We can formulate how the probability of a CFLOS might be given for any viewing path:

$$P'_T = P'_v P'_H = \prod_{i=0}^{18} \left(f'_i\right)^{z_i/\lambda_v} \prod_{i=0}^{18} \left(f'_i\right)^{x_i/\lambda_H} \tag{10}$$

Equation 12 is speculative; in addition to not knowing the value of λH we also do not know the functional relationship between the coefficient of correlation (r) and x/λH. Also, equation 12 has the total path length (the sum of all of the xi and zi values) greater than the line-of-sight path length from the sensor to the object.

Therefore initially, we examined the effect on the CFLOS probability (P') assuming that λ_H = λ_v = 1 km and that the CFLOS probability was only affected by the line-of-sight path length. This enabled us to estimate a CFLOS probability (P') over an arbitrary path through the atmosphere and is given by:

$$P' = \prod_{i=0}^{18} \left(f'_i\right)^{l_i} \tag{11}$$

In equation 13 l_i is the path length through the vertical layer between i and i+0.99 km taking in account the sphericity of the earth. The value of l_i can be less than 1 km for the layer where the sensor or object are located and can be much greater than 1 km for path lengths which traverse through an entire layer that are near horizontal. l_i is zero when a layer is entirely below the viewing path.

Equation 13 underestimates CFLOS probability because it overestimates the effect of the decrease in the probability when viewing with a horizontal component. However, equation 13 is a starting point for comparing various geographic regions.

Figure 4 shows the CFLOS probability at Kwajalein as a function of Sensor Standoff Distance ($\mathbf{X_{SO}}$). For this example the sensor is at a height of 12 km and the object being viewed is at an altitude of 100 km above

sea level. Three curves are shown for λ_h = 1, 10, 100 km. For λ_h = 1 km equation 13 is used to calculate the CFLOS probability (P') and for λ_h = 10 and 100 km equation 11 is used to calculate (P'_T).

From observational experience for aircraft at Kwajalein it is our belief that P' for λ_h = 1 km underestimates the CFLOS probability. On the other hand our impression is that P'_T for λ_h = 10 km overestimates the CFLOS probability. This is perplexing because a horizontal characteristic length scale of 10 km is small with respect to the widespread coverage of cirrus cloud in this area. It is hard to visualize how a 10 km horizontal displacement could be sufficient that the cloud conditions could be uncorrelated.

This leads us to conclude that our model given in equation 12 is oversimplified.

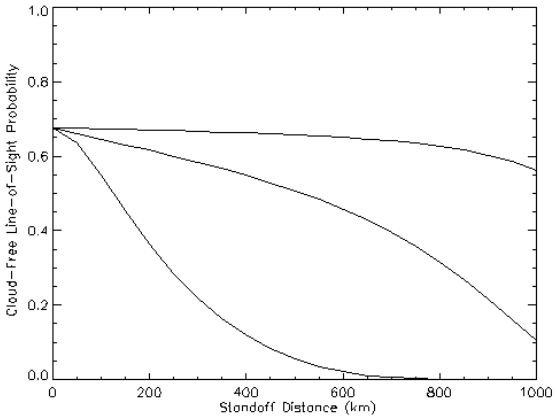

Figure 4: CFLOS Probability versus Standoff Distance for Kwajalein Atoll (Nε ≥ 0.1). The Sensor Height (h_s) is 12 km the Object Height (h_o) is 100 km. The lowest curve is for characteristic length scale (λ_h) of 1 km using equation 13 (P'). The other two curves are for λ_h = 10, 100 km using equation 12 (P'_T).

The CFLOS probability for viewing an object above the atmosphere, in this case at 100 km MSL, is examined for three sensor heights of 0, 12, and 15 km MSL (**Figure 5**). A zero height is chosen because of its interest for ground observation, a height of 12 km (39,372 ft) is chosen because this height is readily obtainable by corporate jet aircraft (i.e. Learjet 36A and Gulfstream-IIB) when at gross weight and operating in ISA (International Standard Atmospheric) conditions. 15 km (49,215 ft) is chosen because it represents an upper certificated maximum operating altitude of production corporate jet aircraft.

Figure 5 shows the CFLOS probability at Kwajalein for viewing an object at 100 km MSL as a function of Standoff Distance (X_{so}) for three sensor heights of 0, 12 and 15 km MSL. The advantage of increasing the sensor height to increase the CFLOS probability is clearly evident when viewing an object above the atmosphere.

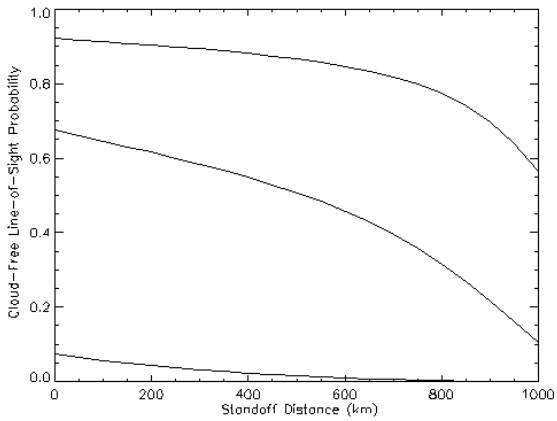

Figure 5: CFLOS Probability versus Standoff Distance for Kwajalein Atoll (Nε ≥ 0.1). The Three Curves are for Sensor Heights of 0 km (Lower Left Curve), 12 km (Middle Curve), and 15 km (Upper Right Curve). The Object Height is 100 km.

If the object of interest for viewing is above the atmosphere, in this case above 19 km MSL, or on the earth's surface then the standoff distance (X_{so}) and object height (h_O) can be combined and presented as a function of the viewing angle (**Figure 6**) with respect to the local horizon at the sensor (θ_{HOR}). **Figure 6** shows the CFLOS probability as a function of θ_{HOR} for three sensor heights of 0, 12, and 15 km.

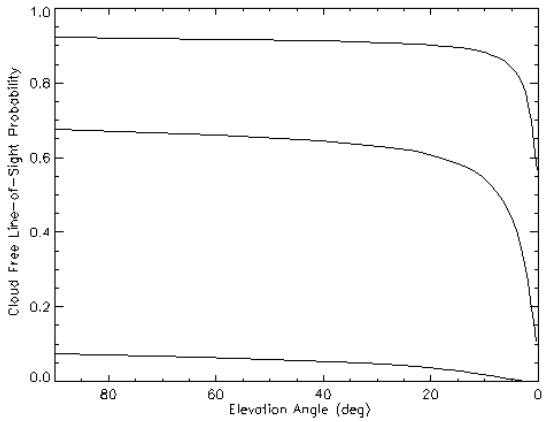

Figure 6: CFLOS Probability versus Viewing Elevation Angle from the Sensor for Annually Averaged Data from the Kwajalein Atoll (Nε ≥ 0.1). The Three Curves are for Sensor Heights of 0 km (Lower Left Curve), 12 km (Middle Curve), and 15 km (Upper Right Curve).

Figure 6 in some respects is a little misleading because it indicates that the CFLOS probability only significantly decreases after the object is below 20° above the horizon. This is true, however, because the last 20° is approximately half of the viewing opportunity.

The next geometric perspective examined is the situation when observing an object that is on the ground (h_o = 0 km) from viewing heights (h_s) of 12 and 15 km.

Figure 7 shows the CFLOS probability as a function of standoff distance.

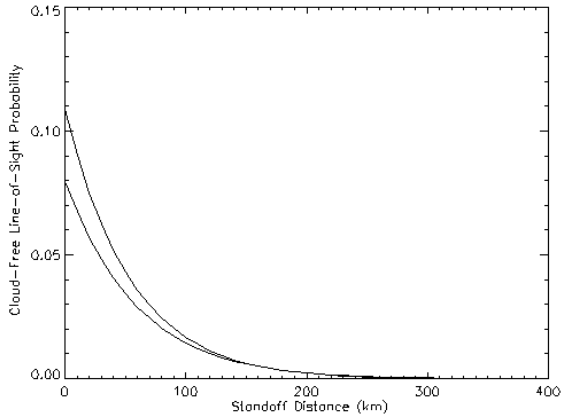

Figure 7: CFLOS Probability versus Standoff Distance for Kwajalein Atoll (Nε ≥ 0.1). The Two Curves are for Sensor Heights of 12 km (Upper Curve), and 15 km (Lower Curve). The Object is on the ground.

Figure 8 shows the CFLOS probability as a function of θ_{HOR} for two sensor heights of 12 and 15 km.

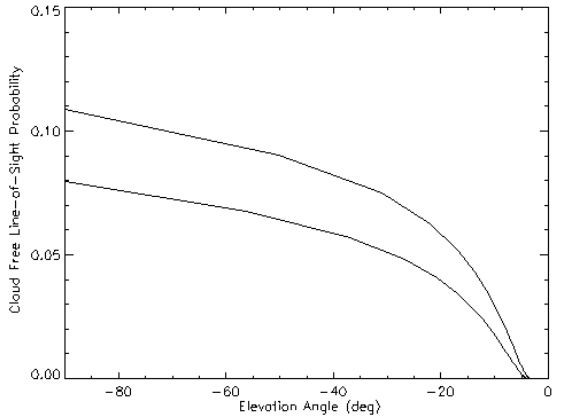

Figure 8: CFLOS Probability versus Viewing Elevation Angle from the Sensor for Annually Averaged Data from the Kwajalein Atoll (Nε ≥ 0.1). The Two Curves are for Sensor Heights of 12 km (Upper Curve), and 15 km (Lower Curve) for an object on the ground.

The next question of interest is to examine how the CFLOS probability varies with geographic region. Two contrasting regions are chosen; Barrow, Alaska (USA) and Lamont, Oklahoma (USA). These sites are chosen because of the Department of Energy (DOE) Atmospheric Radiation Monitoring (ARM) sites there. Barrow's climate can be classified as having an arctic maritime or polar tundra climate and Lamont's climate is classified as humid subtropical.

Figure 9 shows the CFLOS probability at Barrow for viewing an object at 100 km MSL as a function of Standoff Distance (X_{so}) for three sensor heights of 0, 12 and 15 km MSL. The large increase in CFLOS probability from viewing from the ground to 12 km is probably related to the presence of predominately level clouds. This is also supported by the small difference between CFLOS probabilities when viewing from either 12 or 15 km.

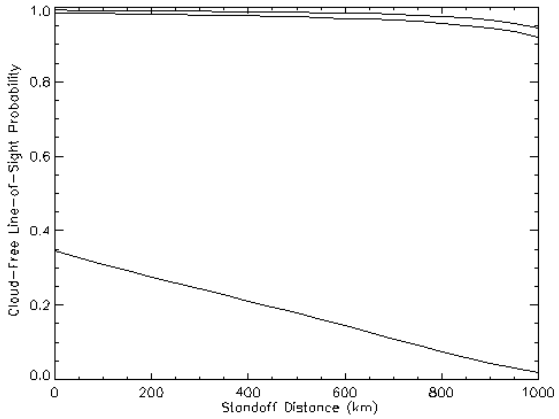

Figure 9: CFLOS Probability versus Standoff Distance for Barrow Alaska (Nε ≥ 0.1). The Three Curves are for Sensor Heights of 0 km (Lower Left Curve), 12 km (Middle Curve), and 15 km (Upper Right Curve). The Object Height is 100 km.

Figure 10 shows the CFLOS probability at Lamont for viewing an object at 100 km MSL as a function of Standoff Distance (X_{so}) for three sensor heights of 0, 12 and 15 km MSL. The CFLOS probability for viewing from the surface at Lamont is greater than that from Barrow. However, for sensor at 12 and 15 km in height the CFLOS probability is less than that for Barrow, indicating the presence of more frequently occurring cloud over Lamont than Barrow.

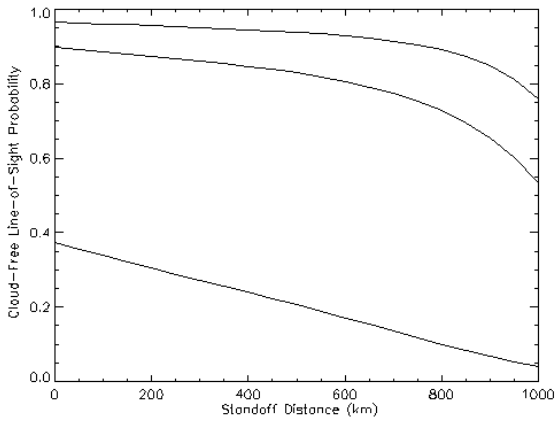

Figure 10: CFLOS Probability versus Standoff Distance for Lamont Oklahoma (Nε ≥ 0.1). The Three Curves are for Sensor Heights of 0 km (Lower Left Curve), 12 km (Middle Curve), and 15 km (Upper Right Curve). The Object Height is 100 km.

Both Barrow and Lamont have better viewing conditions than Kwajalein for all heights thus indicating that these locations have less cloud than Kwajalein.

4. SUMMARY

A method has been developed to estimate the cloud-free-lines-of-sight (CFLOS) from a worldwide satellite-based cloud climatology developed by Dr. Don Wylie at the Space Science and Engineering Center at the University of Wisconsin. This knowledge is of use to those who need to know the probability that cloud might obscure the view of an airborne sensor and the clear path lengths that might be encountered.

The method has application to any region covered by the climatology; data for Kwajalein Island, Barrow, AK, and Lamont, OK were examined. CFLOS probabilities as functions of standoff distance and viewing elevation angle were examined. Even though the estimates have some drawbacks, they can easily be used to compare expected viewing conditions over many different geographic regions.

REFERENCES:

Bedrick, M, K. Swanson, L. Rose, and B. Morrison, 2001: Initiation of a high resolution tropical cloud climatology. Preprints, 11th Conf. On Satellite Meteorology and Oceanography, Madison, WI, Amer. Meteor. Soc., 149-152.

Rose, R.L., M. Bedrick, K. Swanson, and B. Morrison, 2001: Limb biases in CO_2 cloud height algorithms with respect to high altitude cirrus. Preprints, 11th Conf. On Satellite Meteorology and Oceanography, Madison, WI, Amer. Meteor. Soc., 126-127.

Wylie, D.P., and W.P. Menzel, 1999: Eight years of high cloud statistics using HIRS, *J. Climate*, **12**, 170-184.

____, _____, H.M. Woolf, and K.I. Strabula, 1994: Four years of global cirrus cloud statistics using HIRS, *J. Climate*, **7**, 1972-1986.

____, _____ 1989: Two years of cloud cover statistics using VAS, *J. Climate*, **2**, 380-392.